



UNIVERSITÀ DI PARMA

ARCHIVIO DELLA RICERCA

University of Parma Research Repository

An integrated approach for tracking climate-driven changes in treeline environments on different time scales in the Valle d'Aosta, Italian Alps

This is the peer reviewed version of the following article:

Original

An integrated approach for tracking climate-driven changes in treeline environments on different time scales in the Valle d'Aosta, Italian Alps / Masseroli, A.; Leonelli, G.; Morra di Cella, U.; Verrecchia, E. P.; Sebag, D.; Pozzi, E. D.; Maggi, V.; Pelfini, M.; Trombino, L. - In: THE HOLOCENE. - ISSN 0959-6836. - 31:10(2021), pp. 1525-1538. [10.1177/09596836211025974]

Availability:

This version is available at: 11381/2899770 since: 2024-12-13T11:05:43Z

Publisher:

SAGE Publications Ltd

Published

DOI:10.1177/09596836211025974

Terms of use:

Anyone can freely access the full text of works made available as "Open Access". Works made available

Publisher copyright

note finali coverpage

(Article begins on next page)

30 January 2025

1 Version accepted for publication
2 Reuse is restricted to non-commercial and no derivative uses

3 The Holocene

4 1–14

5 © The Author(s) 2021

6 Article reuse guidelines:

7 sagepub.com/journals-permissions

8 DOI: 10.1177/09596836211025974

9 journals.sagepub.com/home/hol

10
11
12 **An integrated approach for tracking climate-driven changes in treeline**
13 **environments at different time scales in Valle d’Aosta, Italian Alps**

14 Anna Masseroli¹, Giovanni Leonelli^{2,3}, Umberto Morra di Cella⁴, Eric P. Verrecchia⁵, David
15 Sebag^{5,6}, Emanuele D. Pozzi¹, Valter Maggi^{3,7}, Manuela Pelfini¹, and Luca Trombino¹

16 1 Department of Earth Sciences “A. Desio”, Università degli Studi di Milano, Milano, Italy;

17 2 Department of Chemistry, Life Sciences and Environmental Sustainability, Università degli Studi di Parma, Parma,
18 Italy;

19 3 Department of Earth and Environmental Sciences, Università degli Studi di Milano-Bicocca, Milano, Italy;

20 4 Environmental Protection Agency of Aosta Valley, ARPA Valle d’Aosta, Saint Christophe, Italy;

21 5 Institute of Earth Surface Dynamics, Faculty of Geosciences and the Environment, Université de Lausanne,
22 Switzerland;

23 6 IFP Energie Nouvelles (IFPEN), Direction Géosciences, Rueil-Malmaison, France;

24 7 Istituto di Geoscienze e Georisorse, Consiglio Nazionale delle Ricerche, Pisa, Italy;

25
26 e-mail and ORCID:

27 anna.masseroli@unimi.it, <http://orcid.org/0000-0002-9845-2608>

28 giovanni.leonelli@unipr.it, <http://orcid.org/0000-0002-1522-1581>

29 u.morradicella@arpa.vda.it,

30 eric.verrecchia@unil.ch, <http://orcid.org/0000-0001-7105-256X>

31 david.sebag@ifpen.fr, <http://orcid.org/0000-0002-6446-6921>

32 lele.pozzi@live.it,

33 valter.maggi@unimib.it, <http://orcid.org/0000-0001-6287-1213>

34 manuela.pelfini@unimi.it, <http://orcid.org/0000-0002-3258-1511>

35 luca.trombino@unimi.it, <https://orcid.org/0000-0002-7714-2686>

36 **Abstract**

37 Both biotic and abiotic components, characterizing the mountain treeline ecotone, respond differently to
38 climate variations. This study aims at reconstructing climate-driven changes by analyzing soil evolution in the
39 late Holocene and by assessing the climatic trends for the last centuries and years in a key high-altitude climatic

40 treeline (2515 m a.s.l.) on the SW slope of the Becca di Viou mountain (Aosta Valley Region, Italy). This
41 approach is based on soil science and dendrochronological techniques, together with daily air/soil temperature
42 monitoring of four recent growing seasons. Direct measurements show that the ongoing soil temperatures
43 during the growing season, at the treeline and above, are higher than the predicted reference values for the
44 Alpine treeline. Thus, they do not represent a limiting factor for tree establishment and growth, including at
45 the highest altitudes of the potential treeline (2625 m a.s.l.). Dendrochronological evidences show a marked
46 sensitivity of tree-ring growth to early-summer temperatures. During the recent 10-yr period 2006-2015, trees
47 at around 2300 m a.s.l. have grown at a rate that is approximately 1.9 times higher than during the 10-yr period
48 1810-1819, one of the coolest periods of the Little Ice Age. On the other hand, soils show only an incipient
49 response to the ongoing climate warming, likely because of its resilience regarding the changeable
50 environmental conditions and the different factors influencing the soil development. The rising air temperature,
51 and the consequent treeline upward shift, could be the cause of a shift from Regosol to soil with more marked
52 Umbric characteristics, but only for soil profiles located on the N facing slopes. Overall, the results of this
53 integrated approach permitted a quantification of the different responses in abiotic and biotic components
54 through time, emphasizing the influence of local station conditions in responding to the past and ongoing
55 climate change.

56

57 **Keywords**

58 Geopedology, soil temperature, dendrochronology, treeline ecotone, climate change, western Italian Alps,
59 late Holocene

60

61 **Introduction**

62 Treeline ecotones, defined as the transition belt in mountain vegetation from closed forest to treeless alpine
63 terrain (Körner, 1999), are one of the most distinctive features in the Alpine landscape and are useful for
64 studying the velocity of landscape dynamics in relationship to climatic changes. Since the ecological dynamics
65 of the alpine treeline ecotone is mainly driven by climate, the treeline is widely considered as a climatic
66 boundary. Indeed, several climatic parameters influence the maximum altitude of the treeline, such as wind,
67 duration of snow cover, frequency and intensity of precipitation, as well as temperature (e.g. Holtmeier and
68 Broll, 2005). Among these parameters, air and soil temperatures are the most important because they impose
69 physiological limits to tree growth. Gehrig-Fasel et al. (2008) suggested that the value of seasonal mean soil
70 temperature can be the most robust indicator for the position of the treeline and calculated the root-zone
71 temperature range at $7 \pm 0.4^\circ\text{C}$ for treelines in the Swiss Alps, not far from the root-zone temperature of $6.7 \pm$
72 0.8°C modeled by Körner and Paulsen (2004) to estimate the treeline position at the global scale.

73

74 Typically, at the site scale, the response time to specific climatic inputs may vary both in biotic and abiotic
75 components, greatly increasing also the possible interactions in the treeline ecosystem. Treelines are related to
76 climate conditions (e.g. Beckage et al., 2008; Burga, 1991; Hughes et al., 2009; Kullman, 2001; Kullman and
77 Öberg, 2009; Leonelli et al., 2011; Scapozza et al., 2010; Vittoz et al., 2008), but their upward shift may be a
78 rather slow process, also under ameliorating climatic conditions, and takes place following fragmented patterns
79 within a region, mainly because of the presence of active geomorphological processes or because of
80 topographic constraints close to the ridges (e.g. Butler et al., 2009; 2003; Leonelli et al., 2016; Macias-Fauria
81 and Johnson, 2013; Masseroli et al., 2016; Virtanen et al., 2010). Actually, the modern treeline altitude at some
82 sites in the European Alps may still be some hundred meters below the historical treelines (e.g. Nicolussi et
83 al., 2005), underlining that the upward recolonization of high-altitude belts may take times up to decades and
84 centuries. On the contrary, under cooling conditions, all trees above a certain altitude may die from one year
85 to the other, causing an immediate downward shift of the treeline.

86

87 Almost immediate responses to climate are also recorded in the tree-ring chronologies of trees growing at the
88 treeline belt, whose growth is strongly limited by climate. Indeed, trees are able to record long series of
89 environmental information with annual resolution in the tree rings, thus acting as natural archives of climate
90 variability through centuries and millennia (Hughes, 2002). Tree-ring chronologies from the temperature-
91 limited environments of the Alps are widely used for reconstructing past climate parameters for periods prior
92 to instrumental data as well as for analyzing the effect of recent global warming on tree-ring growth (e.g.
93 Büntgen et al. 2005, 2011; Coppola et al. 2012, 2013; Corona et al. 2010). Tree-rings may therefore be
94 considered as a useful tool for studying the temporal dynamics of climate at local and regional scales, with
95 annual resolution taking also into account disturbance factors. Moreover, analysis and dating of tree rings from
96 buried logs located above the treeline allow tree growth rates and trends to be compared in different time
97 periods, as well as the reconstruction of previous environmental conditions including the past timberline
98 position (e.g. Nicolussi et al., 2009; Pelfini et al., 2014).

99

100 Although, soil responses to changing climate are a long-term process (Holtmeier and Broll, 2018), the ongoing
101 climatic change, and the consequent altitudinal upward shift of the vegetation belts in mountain areas, may
102 induce the shift of the linked soil processes (e.g. brunification, podzolisation, cryoturbation; Chersich et al.,
103 2015) with century-long response times. For example, the podzolisation line, which is partly related to
104 acidification by the coniferous tree litter, may advance to higher altitude due to the upward shift of the
105 timberline, the boundary of the podzolisation domain. The ongoing climate change, affecting soil temperature,
106 moisture, and snow cover, may influence soil weathering and carbon and mineral balance (Dawes et al., 2017;
107 Egli and Poulénard, 2016; Freppaz and Williams, 2015; Hagedorn et al., 2010), causing a modification of soil
108 properties (e.g. water supply, decomposition, and plant-available nutrient supply) that may affect vegetation
109 growth and colonization (Holtmeier and Broll, 2007; Müller et al., 2016; Sullivan et al., 2015). In turn, tree

110 vegetation itself influences pedogenesis and thus, soil nutrient conditions, by amount, coverage, and quality of
111 litter (Holtmeier and Broll, 2007; Phillips and Marion, 2004). However, the mosaic of soil types that
112 characterizes the treeline ecotone is also closely related to the varying conditions of the local topography.
113 Pronounced dissimilarities exist between soils developed at sites with variable topographic conditions (e.g.
114 exposure, relief forms and gradients; Egli et al., 2010; Holtmeier and Broll, 2018; Masseroli et al., 2020), thus
115 influencing the soil response to climate change. Despite there are no treeline-specific soil types in the temperate
116 mountains (Holtmeier and Broll, 2018), the study of soil properties and characteristics proved to be a useful
117 tool for the investigation and reconstruction of the response of sensitive environments to the past and ongoing
118 climate changes (D'Amico et al., 2016, 2019), as they are the results of the interactions between different
119 environmental factors (i.e. climate, organic activities, relief, parent material, and time; Jenny, 1941).

120

121 In order to assess the past and ongoing environmental evolution at different time-scales in a key high-altitude
122 climatic treeline, we analyzed air/soil temperature data collected over four years of observations (daily scale,
123 present conditions), tree-ring growth (secular scale), and soils (for collecting long-term environmental
124 information) at the Becca di Viou mountain in the Aosta Valley Region (western Italian Alps). Since the
125 climatic treelines in high mountains are highly sensitive to climate and environmental changes, the main aim
126 of this research is to reconstruct the past environmental changes that occurred through time at the Becca di
127 Viou study site, in order to better understand the biotic and abiotic responses to the climatic inputs through
128 time, compared to the more recent climate conditions.

129

130 **Study area**

131 The study area presents one of the highest treelines in the Aosta Valley region and is characterized by extensive
132 mass wasting deposits and patchy stabilized Alpine grassland (Figure 1a, b). This latter is more widespread in
133 the west oriented slope portion, probably due to the presence of a barn and an alpine pasture, where cows graze
134 during summertime, located about 200 m below the forest-treeline boundary (at 2080 m a.s.l.). In the upper
135 portion of the area, from 2700 m a.s.l. and above, the site is characterized by rock faces covering more than
136 90% of the total surface. At lower altitudes, active talus slopes and rockfall deposits characterize the whole
137 treeline belt down to 2300 m, covering up to approximately 40% of the total surface with unconsolidated debris
138 (Leonelli et al., 2011). The low activity of geomorphic processes allows soil formation and colonization of
139 herbaceous and tree vegetation where consolidated deposits are present, resulting in the establishment of
140 continuous open forests of European larch (*Larix decidua* Mill.) in the lower portion of the area and of sparse
141 trees towards the highest altitudes.

142

143 The Becca di Viou study site is located in the Austroalpine geological domain. In the study area, the Mont
144 Mary unit emerges. In this area, an undifferentiated polymetamorphic complex (MMY), mainly composed of
145 paragneiss with relic texture and assemblages of pre-Alpine age and locally displaying mylonitic textures,

146 metapegmatites (MMYb), and paraschists alternating with gneissic pegmatite (MMYc; Dal Piaz et al., 2010),
147 outcrop.

148

149 In the study area, a low degree of development characterizes the soils, which are mainly Leptosol, and in some
150 cases, with a surface layer rich in humus (Umbrisol) including a lot of coarse fractions, a typical feature of
151 high mountain areas. In the lower altitude slope portion, soils are also of Regosol type (Carta Ecopedologica
152 d'Italia 1:250000, Geoportale Nazionale, 2013,
153 http://wms.pcn.minambiente.it/ogc?map=/ms_ogc/WMS_v1.3/Vettoriali/Carta_ecopedologica.map).

154

155 The climate in the region has a semi-continental temperature regime (Dfb climate type following the Köppen-
156 Geiger classification (Peel et al. 2007)). According to the meteorological records in the valley bottom close to
157 the study site (at the Saint Christophe meteorological station (545 m a.s.l.); ARPA Valle d'Aosta) and during
158 the period 1995-2012, the temperature data display a winter minimum in January (-0.4°C) and a summer
159 maximum in July (21.7°C), with an annual variation in temperature slightly over 22°C. Regarding rainfalls,
160 they are scarce in the main valley (approximately 680 mm) but more abundant at the high altitudes of the
161 treeline (1000–1200 mm; Mercalli et al., 2003), mainly occurring during summer months.

162

163 Concerning the vegetation of the study area, Norway Spruce (*Picea abies* (L.) H. Karst) and Scot Pine (*Pinus*
164 *sylvestris* L.) forests dominate the belt under 1900 m a.s.l., whereas the closed mixed forest, dominated by
165 European Larch and Swiss stone pine (*Pinus cembra* L.), reaches higher altitude (about 2300 m a.s.l.;
166 Forestazione-foreste di protezione, Geoportale Valle d'Aosta, 2013,
167 http://geonavsct.partout.it/pub/GeoForeste/index.html?funzione=GF_PROTE). Above the timberline, the area
168 is characterized by a semi-natural treeline ecotone, mainly composed of European larch. In 2008, the treeline
169 was located at an average altitude of 2515 m a.s.l, while the species line of the European larch was found at
170 2545 m a.s.l. in 2009 (Leonelli et al., 2011; Figure 1b). However, up to high altitudes, there are several sparse
171 portions of alpine grassland and shrubs.

172

173 **Material and Methods**

174 *Monitoring of air and soil temperatures*

175 From October 2008 to October 2012, air and soil temperatures were monitored at the treeline belt (Lower
176 Treeline; at 2345 m a.s.l.) and in the area above. Only the soil temperature was monitored at higher altitudes,
177 i.e. at the tree species line (SL; two datalogger at 2545 m a.s.l.) and at the potential treeline (PT30; 2625 m
178 a.s.l.), whose altitude was estimated by considering the occurrence of > 100 days with an air temperature above
179 5°C along a 30-yr period (1975–2004; Leonelli et al., 2011). The five dataloggers of ARPA Valle d'Aosta
180 (HOBO Pro Series; ONSET 1998) recorded air and soil temperatures every 10 to 30 minutes: the recording
181 rate was set according to the datalogger memory capacity. The air temperature datalogger was protected by a

182 sun shield, whereas the soil dataloggers were included in stagnant boxes and the sensors put at 10 cm-deep
183 from the ground surface. Although some technical problems arose during the monitoring period (low battery
184 levels, cable disruption, malfunctioning), high-resolution soil and air temperature changes were obtained for
185 each of the four growing seasons from 2009 up to 2012. These data were used for characterizing soil
186 temperature conditions in the upper portion of the soils of the study area, and for comparing the current
187 temperature conditions at the study site with references to treeline temperature found in the literature.

188

189 *Tree-ring chronology construction from time series*

190 Twenty-four old, living, and standing trees of European larch were sampled in the open-forest belt between
191 2250 and 2350 m a.s.l., by taking two cores per trees using a Pressler's increment borer. Samples were prepared
192 with standard techniques gluing the cores on wood supports and preparing transversal surfaces by means of a
193 plane sanding machine. Tree-rings widths were measured on each core by means of a LINTAB connected to
194 a computer, using the TSAP-Win software (RINNTECH, Heidelberg, Germany): overall, 48 raw individual
195 growth series were obtained. Each growth series was visually and statistically cross-dated with the other
196 growth series from the same tree and with the growth series from the other trees, thus eliminating any potential
197 dating error. A growth series was eliminated because of anomalous growth patterns with respect to the other
198 series. The COFECHA program was used for the statistical cross-dating within and between trees, whereas,
199 the RCSsigFree_v.45 program was run for the construction of a "signal-free" chronology (Melvin and Briffa,
200 2008; both software, www.ldeo.columbia.edu). We adopted the signal-free RCS standardization approach and
201 applied age-dependent spline smoothing (with initial stiffness of 50 yr) for detrending the individual series
202 (Melvin and Briffa, 2014). The signal-free RCS approach mitigates the potential "end effect" bias found in the
203 simple RCS due to the potential conservation of the 20th century growth-increase signal when calculating the
204 regional curve based only on living trees.

205

206

207 *Detection of the climate signal*

208 The detection of the climate signal recorded in the site chronology was performed using a correlation function
209 approach. The site chronology was analyzed against monthly and seasonal values of temperature for the grid
210 cell 45.75 N, 7.25 E comprising the study area (CRU TS Version: 4.01, Harris et al., 2014). Monthly variables
211 from June of the year previous to growth up to September of the year of growth were selected together with
212 aggregate variables of August-to-October (ASO-1) of the year previous to growth and June-to-August (JJA)
213 of the year of growth. Moreover, a linear regression analysis of the standard chronology on summer (JJA)
214 temperature was performed in order to investigate the spread of the points along the regression line and the
215 signal strength. The same correlation analysis was performed also using precipitation variables (not shown).

216

217 *Soil sampling*

218 Seven soil profiles were described, according to Jahn et al. (2006), and sampled slightly below the current
219 treeline at an altitude ranging from 2100 m a.s.l. to 2400 m a.s.l. (Table 1). An altitudinal transect of three soil
220 profiles (BV16/01, BV16/02 and BV16/03), ranging from 2300 m a.s.l. to 2400 m a.s.l., was located on the
221 right portion of SW slope of Becca di Viou, while another altitudinal transect of three soil profiles (BV16/04,
222 BV16/05 and BV16/06), ranging from 2325 to 2370, was placed on the left portion of SW slope of Becca di
223 Viou (Figure 2). As a comparison, one soil profile (BV16/07), located at 2110 m a.s.l., was excavated in a
224 forested area (Figure 1b; Table 1). For each soil profile, coordinates were recorded using a GPS device and
225 from each identified soil horizon, between 0.5 to 2 kg of material were sampled for laboratory analyses (Avery
226 and Bascomb, 1982; Cremaschi and Rodolfi, 1991; Gale and Hoare, 1991).

227

228 *Soil mineral matrix analysis*

229 Soil pH was estimated on fine earth using a soil solution ratio of 1:2.5 (soil: distilled water). Particle size
230 distributions were determined after sample pretreatment with H₂O₂ (130 volumes) using a combined method
231 consisting of sieving for particles between 2000 µm and 63 µm, and aerometry (Casagrande aerometer method)
232 for the finer particles (< 63 µm).

233 Acid ammonium oxalate and dithionite-citrate-bicarbonate were used to extract iron and aluminum from
234 amorphous oxides and hydroxides (“active” forms, Fe_o and Al_o), and iron and aluminum form non-silicate
235 forms (“free” iron, Fe_d and Al_d), respectively (Ministero delle Risorse Agricole Alimentari e Forestali, 1994).
236 The amount of solubilized iron and aluminum in the supernatant was determined by means of a 4100 MP-AES
237 (Agilent) after the appropriate dilutions. Since no data have a %RSD (Relative Standard Deviation) of
238 concentration > 3.5 and/or a not detectable clear peak, all results were considered valid, whereas the data close
239 to the detection limit of the instrument were approximated to the minor concentration detectable (< n in Table
240 2). In addition, both the iron activity index (Fe_o/Fe_d) and the illuviation (podzolization) index (Al_o+½Fe_o) were
241 calculated (IUSS Working Group WRB, 2015); the amount of crystalline iron oxides (Fe_{cry}) was calculated by
242 the difference between the dithionite- and the oxalate-extractable Fe (Fe_{cry}= Fe_d-Fe_o; Bascomb, 1968;
243 Cremaschi and Rodolfi, 1991; Zanelli et al., 2007).

244

245 *Soil organic matter analysis*

246 Total organic C (C_{org}) and N (TN) contents were determined using the Walkley-Black (Walkley and Black,
247 1934) and Kjeldahl methods (Kjeldahl, 1883), respectively. The OM properties were obtained by thermal
248 analysis performed with a Rock-Eval® 6 pyrolyser (Vinci Technologies, France). About 60 mg of crushed
249 material, previously sieved (< 2 mm), were analyzed for each horizon. Standard parameters – Total Organic
250 Carbon (TOC), Hydrogen Index (HI) and Oxygen Index (OI) – were calculated according to the conventional
251 procedure (Behar et al., 2001; Lafargue et al., 1998). In addition, two thermal parameters related to the most
252 reactive fraction of soil OM (i.e. pyrolyzed carbon) were computed according to Sebag et al. (2016). By
253 construction, the R-index relates to the thermally resistant and refractory pools of soil OM, while the I-index

254 is related to the ratio between the thermally labile and resistant pools (see Sebag et al., 2016 for details). As
255 derived from a mathematical construct, these two indexes may be inversely correlated along a constant line
256 ("*humic trend*" in Sebag et al. 2016; "*decomposition line*" in present study) when OM stabilization results
257 from progressive decomposition of organic components according to their biogeochemical stability. Then, a
258 decrease in labile pools result in a concomitant increase in more thermally stable pools, as observed in compost
259 samples and undisturbed soil profiles (Albrecht et al., 2015; Matteodo et al., 2018; Schomburg et al., 2018,
260 2019; Sebag et al., 2016). Matteodo's dataset composed of 46 soil profiles selected across various eco-units in
261 Swiss Alps (Matteodo et al., 2018) was used for comparison. Finally, the stable carbon and nitrogen isotope
262 abundances in the samples were determined using a Thermo Scientific Delta V device. The $\delta^{13}\text{C}$ and $\delta^{15}\text{N}$
263 values are reported relative to the Vienna Pee Dee Belemnite standard (VPDB) and air- N_2 , respectively.
264 Laboratory standards were calibrated relative to international standards.

265

266 **Results**

267 *Air and soil temperature results*

268 The monitoring of air temperatures at the study site gave ranges between approximately $-15\text{ }^\circ\text{C}$ (for January
269 2010 and 2011 and for February 2012) and $17\text{ }^\circ\text{C}$ (usually reached in August; Figure 2) during the recent
270 period. Soil temperatures, instead, showed markedly higher minimum temperatures, close to $0\text{ }^\circ\text{C}$ during winter
271 for all dataloggers, except for the *Ts Species line 2*, which reached approximately $-3 - -4\text{ }^\circ\text{C}$. As regards
272 maximum soil temperatures, some dataloggers recorded values higher than air temperatures: the datalogger *Ts*
273 *potential treeline 30 yr* usually overpassed the temperature of $20\text{ }^\circ\text{C}$ in August; the *Ts species line* reached
274 $19.9\text{ }^\circ\text{C}$, whereas the other dataloggers reached approximately $17\text{ }^\circ\text{C}$ (Figure 2). For what concerns the average
275 soil temperature during the growing season, values slightly exceeded $11 - 12\text{ }^\circ\text{C}$, except for *Ts Species Line 2*
276 that recorded lower temperature values at approximately $8.5 - 9.5\text{ }^\circ\text{C}$. The growing season lengths (Körner
277 and Paulsen, 2004) have only been evaluated for the complete periods of 2009, 2011, and 2012, and resulted
278 in 166 ± 15 days.

279

280 Temperature and precipitation variations by the grid cell $45.75\text{ N} - 7.25\text{ E}$ over the common period 1902-2015
281 (Fig. 3; CRU TS Version: 4.01, Harris et al., 2014) display a visible increasing trend for both variables. The
282 mean JJA temperature is $8.8^\circ\text{C} \pm 1\text{ }^\circ\text{C}$ and shows a local maximum in the 1940s and a recent increasing trend
283 in temperature since the late 1970s. According to the linear trend calculated over 1902-2015, this temperature
284 variable exhibits an increasing rate of $+1.6^\circ\text{C}$ in 100 yr. Precipitation of the water year (October of the previous
285 year to September) is 1827 ± 258 mm in average, with maxima reached during summer (JJA; 524 mm) and
286 minima during winter (DJF; 403 mm). According to the linear trend calculated over 1902-2015, the October-
287 to-September precipitations (i.e. a water year) have an increasing rate of $+64.7$ mm in 100 yr. By analyzing
288 the seasonalized variables (not shown), this trend is mainly due to an increase in winter precipitations (DJF;

289 +38.6 mm) and summer precipitations (JJA; +16.0 mm), whereas spring precipitations show a decreasing trend
290 (MAM; -5.9 mm).

291

292 *Tree-ring chronology*

293 The Becca di Viou tree-ring chronology spans over 204 years from 1812 to 2015 and it holds a good signal
294 stability underlined by the EPS index value, i.e. $EPS > 0.85$ (Briffa and Jones, 1990) since 1852 (Figure 3).

295 Slightly lower values of $EPS > 0.76$ are reached since 1823. The chronology showed periods of reduced tree-
296 ring growth during the 1810-1820 period, the first years of the 1880s, the 1905-1915 and 1975-1980 periods.
297 Although discontinuous, the recent positive trend of markedly higher tree-ring growth rates started during the
298 1980s, with the last 10-yr period presenting an average growth index value of approximately 1.9 times the
299 growth index during the 10-yr period of minimum growth in the chronological record (i.e. 1810-1819).
300 According to the linear trends calculated on z-scores over the 1902-2015 period, the tree-ring index has an
301 increasing rate that is comparable, and higher, to that of the temperature record (+1.65 and +1.56, respectively,
302 over 100 yr) (Table in Fig. 3).

303

304 An expected dependence of growth patterns during summer months is observed when comparing the
305 temperature record with the associated dendrochronological data (Figure 4a). Temperatures of the late summer
306 and early autumn, (August-to-October), mainly influence tree-ring growth in the following growing season.
307 By analyzing seasonal variables aggregating couples of months, the dendrochronology data show correlations
308 up to $r = 0.67$ ($p < 0.001$) with JJA and 0.49 ($p < 0.001$) with ASO-1. For precipitation, we found a statistically
309 significant correlation, $r = -0.29$ ($p < 0.01$) only with June precipitation.

310 The regression of the ring-width index on the JJA variable, shows a clear dependence of tree-ring growth on
311 the summer temperatures, with this climate variable explaining up to 45% of the tree-ring growth variability
312 (Figure 4b). Therefore, the tree-ring growth patterns recorded in the dendrochronological data well follow the
313 summer (JJA) temperature variability through time.

314

315 *Soil matrix analysis*

316 The studied soil profiles assume variable thicknesses (usually 30 to 60 cm) depending on the altitude range,
317 vegetation cover, and geomorphological settings. The maximum thickness is found in soils that evolved under
318 forest vegetation and the minimum thickness in soils developed at the treeline ecotone, with the exception of
319 profile BV16/02, which is rather deep (75 cm), even if located at the treeline ecotone. Horizon colors show a
320 clear uniformity in the area, particularly in regards to the hue values, which are never different from 10 YR or
321 2.5 Y. Soil structure is moderately expressed and it is mainly characterized by granular aggregates, or less
322 frequently by subangular blocky aggregates (Supplemental Material Table S1).

323

324 Analyses of particle size distributions (PSD) carried out on soil profiles showed a marked presence of coarse
325 material. The gravel fraction varied between 3.0% and 65.1%. Among the fine earth, the most representative
326 particle size fraction is silt, which ranges from 15.0% to 62.4% of total weight (Figure 5), whereas the amounts
327 of sand and clay, between 8.0 and 32.9%, and between 0.2 and 15.8%, respectively. All the analyzed soil
328 profiles showed a decrease of the coarse component from bottom to top (Figure 5; Supplemental Material
329 Table S2).

330

331 Like in all analyzed profiles, the BV16/02 profile displays a coarse fraction content increasing with depth, as
332 well as a progressive decreasing trend in clay. However, its cumulative PSD curves (Supplemental Material
333 Figure F1) show two distinct families of grain populations: one includes the superficial horizons (O and AC)
334 and another the deeper horizons (2AB, 2Bw and 2BC). Moreover, the presence of a small stone line in the
335 field, characterized by elongated subangular decimetric clasts, was observed between the AC and 2AB
336 horizons.

337

338 All soil horizons' $\text{pH}_{\text{H}_2\text{O}}$ values range from 4.6 to 5.6 (Figure 5). Almost all measured pH vary by only a < 0.5
339 pH unit along the profiles.

340

341 Among the different forms of extractable iron, the free iron oxides (Fe_d) are the most common in the analyzed
342 horizons: the total contents of free iron oxides (Fe_d) range from 3.23 to 19.03 g/Kg. However, the values of
343 amorphous iron oxides (Fe_o) are slightly lower, ranging between < 0.9 and 13.64 g/Kg. For both forms of
344 extractable iron, particularly high values are observed in BV16/02 2AB and BV16/03 BC horizons (Table 2).
345 On the contrary, the different forms of extractable aluminum, i.e. free aluminum oxides (Al_d) and amorphous
346 aluminum oxides (Al_o), reached values between 0.99 and 5.82 g/Kg and between 0.63 and 6.01 g/Kg,
347 respectively. The crystalline iron oxides Fe_{cry} content was very variable: in profile BV16/01, Fe_{cry} contents are
348 low (1.65-3.3 g/Kg), whereas in profiles BV16/04 and BV16/05 the Fe_{cry} reached higher values, with a peak at
349 10.19 g/Kg in the BV16/04 AC horizon. The comparison between Fe_{cry} and Fe_o trends (Figure 6) underlines
350 the presence of a trend between these two forms of iron in the more developed profiles. Moreover, a Fe_o peak
351 in the B horizons is also clear. High values for the iron activity ratio (Fe_o/Fe_d) are found in the BV16/02 2AB
352 (0.72), BV16/03 BC (0.86) and BV16/07 BC2 (0.68) horizons, whereas in the other horizons the iron activity
353 index ranged from about 0.2 to 0.5 (Table 2). Finally, the results of the podzolisation index $\text{Al}_o + \frac{1}{2} \text{Fe}_o$ meet
354 the conditions of podzolisation processes in the BV16/02, BV16/03 and BV16/07 profiles (IUSS Working
355 Group WRB, 2015; Table 2).

356

357 *Soil organic fraction analysis*

358 Regarding the Total Organic Carbon (C org.) and Total Nitrogen (TN) contents, soil profiles are characterized
359 by decreasing C org. and TN contents with depth (Figure 5, Supplemental Material Table S2). In more details,

360 the absolute quantities of C org. are variable depending on the type of profile and its depth (Figure 5). As
361 expected, the highest content of C org. is found in superficial horizons, where values range from 55.8
362 (BV16/03) to 135 g/kg (BV16/07). In the superficial horizons, the highest contents of TN are found in the
363 BV16/01 O (10.2 g/Kg) and BV16/05 O (10.3 g/Kg). Finally, the C/N ratio have values ranging between 8.8
364 and 14.7 in the superficial horizons.

365

366 According to the Rock-Eval pyrolysis analysis (Figure 7), the HI vs OI diagram displays a clear distinction
367 between the surficial O and A horizons (at the top left), characterized by high values of HI inherited from fresh
368 biological inputs, and the deeper B and C ones (at the bottom right), characterized by high values of OI related
369 to transformed pedogenic and petrogenic organic matter (Figure 7a). The horizons belonging to the buried soil
370 (BV16/02) have the highest OI values. Moreover, the thermal stability of the organic matter increases with
371 depth in the analyzed soil profiles: the TOC decreases from the topsoil to the subsoil mineral layers and the R
372 index increases, particularly in the horizons belonging to the buried soil (BV16/02 2AB, 2Bw and 2BC; Figure
373 7b, c). Moreover, the buried horizons (BV16/02 2AB, 2Bw and 2BC), placed at the bottom right in the I/R
374 diagram, are separated from the other horizons and, are not exactly located on the “*decomposition line*” (see
375 Sebag et al., 2016) contrary to the other studied horizons (Figure 7b).

376

377 Furthermore, the $\delta^{15}\text{N}$ trend in the profile BV16/02 shows a peculiarity: while in all other profiles the $\delta^{15}\text{N}$
378 increases with depth (Figure 8b), a trend inversion is found in this profile in correspondence with the 2AB and
379 following horizons (2Bw and 2BC). The $\delta^{13}\text{C}$ distribution shows a trend inversion, not only in the BV16/02
380 but also in the BV16/01, BV16/05 and BV16/07 profiles (Figure 8a). However, the BV16/02 is the only profile
381 showing a marked trend inversion and a negative $\Delta\delta$ (isotopic enrichment for each profile with reference to
382 the first horizon), along the profile for both $\delta^{13}\text{C}$ and $\delta^{15}\text{N}$ (Figure 8c, d).

383

384 **Discussion**

385 The multidisciplinary analysis carried out at the high-altitude climatic treeline environments of Becca di Viou
386 mountain allows the environmental changes characterizing the area to be reconstructed through time.
387 Moreover, the results show that the abiotic and biotic components at the treeline ecotone respond to the past
388 and ongoing climate changes at different time scales, also according to local station conditions.

389

390 As in other Alpine sites, the ongoing climate change in the study area is principally observable in rising air
391 temperatures. Temperatures display a visible increasing trend for the period 1902-2015. The mean JJA
392 (growing season) temperatures particularly show a local maximum in the 1940s and a recent increasing trend
393 since the late 1970s, exhibiting an increasing rate of +1.6°C in 100 yr. The JJA mean air temperatures increase
394 (+1.6°C in 100 yr) over the 1902-2015 period was also observable and of comparable magnitude in the tree-
395 ring chronology , which show higher values during the recent years, starting from the 1980s. Although

396 correlations computed over long time periods with aggregate temperature variables may underline climate-
397 growth responses in high altitude sites, often, over shorter time periods and using monthly variables may reveal
398 decreasing correlation values in recent years, especially with June temperature. Decreasing trends in
399 correlation values for early summer temperature and increasing negative trends for early summer precipitation
400 were in fact obtained, e.g., in some studies carried out on Swiss stone pine and European larch in the Alpine
401 treeline ecotone (Leonelli et al., 2009; Coppola et al., 2012;). These trends may be related to the so called the
402 “divergence problem” - DP (Büntgen et al., 2008), causing a lack of correlation with climatic variables. The
403 DP is closely related to the 20th century temperature’s increase and can be attributed to the growing season
404 prolongation as well as to local and global issues (D’Arrigo et al., 2008), including pollution, drought stress,
405 etc. Numerous studies have reported an extension of the growing season in Europe due to the recent
406 temperature increase (Menzel and Fabian, 1999; Menzel et al., 2006; Sparks and Menzel, 2002; Walther et al.,
407 2002).

408

409 Indeed, the prolonged growing season and the warmer temperature conditions during the growing season has
410 likely caused an upward shift of the vegetation belts, and of the treeline at the study site (Leonelli et al., 2011).
411 But our analysis of soil temperature showed that the treeline could potentially reach even higher altitude than
412 the present-day position. Indeed, the average soil temperatures, recorded by all dataloggers (including the ones
413 at the Species Line) during the growing season (Figure 2), are higher than the reference soil temperature of 7°
414 C for the treelines in the Swiss Alps (Gehrig-Fasel et al., 2008). Moreover, when comparing our results for the
415 growing-season soil temperatures at the treeline with those proposed by Körner and Paulsen (2004) for the
416 “Cool temperate W. Alps”, the soil temperatures at Becca di Viou reached higher mean values associated to a
417 longer growing season.

418

419 Both the radial growth of trees and tree recruitment are influenced positively by the increasing of temperature
420 and precipitation rates but the patterns and the time of their responses may be different (Wang et al., 2006).
421 Treeline advance may depend upon the coincidence of favorable conditions over sufficient years to permit
422 establishment, growth, and survival. Moreover, treeline dynamics are affected by site and microsite conditions
423 (e.g. microclimate, topography, soil, geomorphological processes) that can mask or modify the impact of
424 climate change. The shift of the vegetation belt caused by the rising of soil and air temperatures, as well as
425 land abandonment, although expected (e.g. Gehrig-Fasel et al., 2007; Vittoz et al., 2008), was not always
426 observed at treeline sites (e.g. Klasner and Fagre, 2002; Mazepa, 2005). Indeed, plant communities are often
427 decoupled from the local climate dynamics, as plants may be influenced by several biotic and abiotic
428 interactions (Malanson et al., 2019).

429

430 The soil response to climate change is even more complex. The analyzed soil profiles show a weak degree of
431 development, likely due to the slope steepness and other disturbance factors, such as erosional/depositional

432 processes, distinctive of mountain environments (Bollati et al., 2019; Legros, 1992; Zanini et al., 2015). The
433 incipient stage of soil development is supported by the preponderant presence of coarse material, typical of
434 Alpine soils on substratum made of debris or moraine deposits (Egli et al., 2001). As in other Alpine contexts
435 (D'Amico et al., 2015; 2009), the influence of parent material in the Becca di Viou study site on soil properties
436 is stressed not only by the particle size distributions, but also by the pH of the soil material (Figure 5). The soil
437 pH displays only little variations throughout the profiles, and the superficial horizons are not characterized by
438 the expected increase in acidity; in this light, the parent material mainly influences soil acidity.

439

440 In addition, Rock-Eval signatures support the weak soil development (Figure 7). Indeed, the OM of the
441 superficial horizons presents a composition (HI, OI) quite comparable to the OM biogenic rich layers, like
442 litter or humus (Matteodo et al., 2018; Sebag et al., 2016). The positions of O horizons in the I/R diagram
443 (separate from the litter) indicate that decomposition processes are active and intense. On the other hand, most
444 of A and B horizons indicate that OM stabilization related to pedogenic processes (i.e. organo-mineral
445 complexation and aggregation; Lehmann and Kleber, 2015) is rather moderate.

446

447 Moreover, spatial heterogeneity and diversity of soil forming factors (Jenny, 1941) influence soil evolution,
448 conditioning the soil response to climate change. An increment of soil development is observable all along the
449 soil toposequences: as in other Alpine soils (Merkli et al., 2009; Egli et al., 2008), the profiles located at higher
450 altitudes are thinner and less developed compared to those at lower elevation. In addition to the vertical
451 zonality, the studied soils showed different properties according to their slope characteristics (i.e. aspect, slope)
452 and geomorphological contexts. The gentler slope, and the less presence of rockfall deposits of the N facing
453 slope than on S facing slope, influenced and still influences the soil development and their characteristics.
454 However, the two soil toposequences seem to be mainly influenced by their aspect. The different aspects of
455 the two slopes affect the climatic parameters (e.g. soil temperature), and therefore soil processes. Among the
456 studied profiles, only those located on the N facing slopes (BV16/01, BV16/02 and BV16/03) show a shift
457 from Regosol to soil with more marked Umbric characteristics, developing a B horizon. These data agree with
458 other studies carried out in the Alps (Egli et al., 2006, 2009, 2010) showing the effect of slope aspect on soil
459 development and characteristics. Egli et al., (2010) found that climatic parameters (e.g. lower temperatures,
460 lower evapotranspiration, higher humidity) of N facing slopes can lead to an accumulation of labile, weakly
461 degraded organic matter, and consequently, to a higher production of soluble organic ligands that enhance the
462 migration (eluviation) of Fe and Al compounds. The different degree of illuviation of amorphous material is
463 testified by the presence in B horizons on N facing slopes of higher concentrations of Al_o and Fe_o compared to
464 those on S facing slopes (Table 2), and by a greater difference of Al_o and Fe_o between the uppermost soil layer
465 and the B horizon on the N facing slope (Egli et al., 2006, 2009). Moreover, Fe_o/Fe_d ratio values, which may
466 indicate both iron illuviation and extreme weathering effects (Waroszeski et al., 2013; Zanelli et al., 2007), are
467 higher in the B horizons of soils located at N facing slopes (Table 2). The values of the $Al_o + \frac{1}{2} Fe_o$ index

468 obtained at profiles BV16/02 and BV16/03, as at profiles BV16/07, seem to indicate a weak evidence, only
469 partially recognizable in the field, of some podzolisation processes (Do Nascimento et al., 2008; IUSS Working
470 Group WRB, 2015; Waroszewski et al., 2013; Table 2). The presence of a weak podzolisation (i.e.
471 cryptopodzolisation) could promote the formation of Umbrisols (protosodic) (IUSS Working Group WRB,
472 2015). Anyway, the podzolisation index of profile BV16/02 is not easy to interpret, since the horizons (AC
473 and 2AB) in which the index meet the condition of podzolisation processes belong to two different pedological
474 units.

475

476 Some of the geopedological aspects mentioned above point out a soil weaker development than expected. This
477 can be viewed as a consequence of unstable geomorphic conditions. On the other hand, this apparent
478 disequilibrium can be explained considering soil as a highly resilient system capable of persisting over time
479 and being able to absorb change and disturbance, still maintaining the same relationships between state
480 variables (Holling, 1973). The studied profiles show a current shift between different pedogenetic processes
481 (i.e. from Regosols to Umbrisols (protosodic)) induced by climate, but with a longer response time than
482 vegetation. Therefore, the analyzed soils provide a realistic understanding of the systems behavior under the
483 ongoing climate change.

484

485 The study of tree-ring growth and soil has also allowed us to collect information about the environmental
486 changes that have occurred in the study area during the past. The high sensitivity of tree-ring growth to summer
487 temperatures (JJA; Figure 4) allowed the growth trends in the chronology to be analyzed in order to reconstruct
488 the past temperature variability, and underlined the presence of a recent positive trend. The site chronology
489 emphasized periods of reduced and enhanced tree-ring growth at the study site. Indeed, in the last year of the
490 chronology, i.e. in AD 2015, the growth index value reaches 2.3 times the growth over the 10-yr period of
491 minimum growth in the chronology (1810-1819), i.e. during one of the Little Ice Age coolest periods (e.g.
492 Lamb, 1995) in the area. Tree-ring growth in the last decade testifies the improved growing conditions for
493 trees and confirms the high increase of air temperature conditions also at the treeline.

494

495 Whereas, the geopedological analyses allow the identification, in the profile BV16/02, of a past instability
496 phase, interposed between two different stability phases and characterized by clearly developed soil units. A
497 particle size discontinuity and a stone line between AC and 2AB horizons testified the presence of two different
498 pedological (sedimentological) units (Figure 5): a buried unit, partially eroded and covered by debris deposits
499 due to gravity processes, which was mainly induced by climatic oscillations or environmental changes (e.g.
500 changes in vegetation cover), and a surficial unit, affected by present-day pedogenesis. The presence of a
501 buried surface in BV16/02 is also highlighted by the results of stable isotopes: increases in $\delta^{15}\text{N}$ (Gerschlauser
502 et al., 2019; Martinelli et al., 1999) and $\delta^{13}\text{C}$ with depth (i.e. in mineral horizons) are expected in soils under
503 C3 vegetation (Balesdent et al., 1993). Whereas, in the BV16/02 profile, there is a marked inversion of both

504 $\delta^{15}\text{N}$ and $\delta^{13}\text{C}$ trends (Figure 8a, b). The $\delta^{15}\text{N}$ values show a trend inversion between AC and 2AB horizons,
505 with first an isotopic enrichment and then a depletion. Other studies (e.g. Schatz et al., 2011) ascribe this
506 variation to different soil organic matter mineralization due to different climatic conditions. In addition, the
507 small $\delta^{13}\text{C}$ variations between superficial and buried units may reflect changes in soil organic matter
508 mineralization (Zech et al., 2007). Moreover, some characteristics of soil organic matter support this
509 interpretation. The Rock-Eval analysis revealed compositional indices (HI, OI) and thermal status (I/R
510 diagram) specific of buried horizons (Figure 7a, b), with values typical of more decomposed and more
511 stabilized organic matter (Sebag et al., 2016).

512
513 It is possible that $\delta^{15}\text{N}$ may be a more sensitive proxy than $\delta^{13}\text{C}$ in order to reconstruct environmental changes.
514 Indeed, $\delta^{15}\text{N}$ is influenced by mineralization processes and especially by N losses, and this isotopic decrement
515 most likely reflects a decrease of N losses due to the reduced SOM mineralization during the formation of the
516 soil (Schatz et al., 2011). In terms of a paleoclimate, this can be attributed to lower temperatures and probably
517 increased precipitations. Moreover, even if results of carbon stable isotopes suggest that C3 plants have been
518 the main vegetation type for the entire time span during which the profile accumulated (the absence of C4
519 plants is typical of temperate and cold environments), the $\delta^{13}\text{C}$ variations remain interesting for the past climate
520 reconstruction. Stevenson et al. (2005) have shown how the $\delta^{13}\text{C}$ gets lighter with increasing rainfall.
521 Therefore, the presence in BV 16/02 of a buried unit characterized by a well-developed B horizon could be
522 related to a past stable climate phase with different environmental and climate conditions interrupted by some
523 changes. According to the stable isotope results, the buried soil can result from dynamics developed under
524 more humid and colder climate conditions, which occurred after the LGM and Late-glacial period (formation
525 period of the glacial deposits in the study area).

526
527 As evidenced from the obtained results, the soil and vegetation responses to climate change have been in the
528 past, and are today, closely linked to various abiotic and biotic factors; these factors will probably influence
529 the environmental response also in the future. Although the temperature data and dendroclimatological
530 evidence underline a marked rise in temperatures in Becca di Viou area, the upward shift of the treeline was
531 and will be likely halted in the next future because of specific geomorphological constraints (Leonelli et al.,
532 2011). Nevertheless, an increase of tree density and an upward shift of the timberline could occur (Klasner and
533 Fagre, 2002), promoting an advance to higher altitude of podsolization processes, which will be partly related
534 to acidification by the coniferous tree litter. In the future, if the increasing temperature and precipitation rate
535 conditions persist, the formation of Podzols (IUSS Working Group WRB, 2015) could happen. Indeed, higher
536 precipitation rate leads to a higher amount of water percolating through the soil profile, thus promoting the
537 migration of organic matter with Al-Fe complexes (Chersich et al., 2015). However, and considering the
538 present day soil resilience, these soil processes shift towards podsolization will take place in an asynchronous
539 time scale, respect to the establishment of the environmental conditions favorable to the podzolization itself.

540

541 In conclusion, this study underlines the importance of a multidisciplinary approach that, taking into
542 consideration different natural archives, allows the study area evolution to be reconstructed in order to
543 understand the complexity of the factors acting at high altitude environments.

544

545 **Conclusions**

546 As previous studies have demonstrated, the treeline at the Becca di Viou site has moved upward of
547 approximately 75 m since 1950 (Leonelli et al., 2011); but further shifts towards higher altitudes are probably
548 constrained by the slow evolution of soils, their scarcity, the topography, i.e. the steep slopes close to the
549 ridges, as well as the presence of extensive gravity processes. Overall, based on a multi-proxy approach, this
550 study emphasized the different response-times involving biotic and abiotic components in high-altitude treeline
551 ecosystems undergoing the same climate inputs through time. As the soil temperature monitoring at the Becca
552 di Viou site has proven, the ongoing temperature conditions at the treeline, and at the species line during the
553 growing season, are already approximately 3°C above the modeled temperature limits of 7°C in the region.
554 Thus, soil temperatures at the current elevations of the treeline, and the species line, do not represent anymore
555 the main limiting factor either for tree establishment or growth at the highest altitudes.

556

557 Changes of climate conditions at the century scale are well recorded in the tree rings that document, with an
558 annual resolution, the growing season temperature conditions, i.e. June and July. The ongoing trend in growth
559 rates underline the exceptional period that high-altitude trees are facing nowadays at this site. In the recent 10-
560 yr period (2006-2015), trees are growing at a rate that is approximately 1.9 times the growth during one of the
561 coolest periods of the Little Ice Age (1810-1819), and 2.3 times for the last tree ring of 2015.

562 Tree rings proved to be a highly sensitive climate proxy with an annual resolution and a rapid response time,
563 whereas treelines shift, and especially soils, showed slower dynamics, being also influenced by other
564 environmental parameters. Soils show a resilience in relationship to the changeable environmental conditions:
565 few variations of pedogenetic processes are in progress and a shift to higher altitude of podsolization processes
566 is only partially visible in the soils located at N facing slope (Umbrisols protospodic).

567

568 Moreover, soil hold information about past environmental conditions, recording both the stability and
569 instability phases. In BV16/02 profile, it is possible to reconstruct the succession of different phases of
570 biostasy, during which the soil developed, and a phase of rhexistasy, during which the soil was eroded and
571 finally buried, likely because of climate variations that occurred during the Holocene.

572

573 **Acknowledgments**

574 The Authors wish to thank the Regione Valle d'Aosta for the sampling permits, Saint-Cristophe and Roisan
575 municipality for the vehicle transit permit, and Roberta Righini for the first assessment of the datalogger

576 temperatures. The authors are grateful to Dr. Compostella and Dr. Ferrari for their assistance in laboratory
577 analyses. Rock-Eval® is a trademark registered by IFP Energies Nouvelles. The authors thank the International
578 Relations from the University of Lausanne who provided travel funds between Italy and Switzerland. The
579 authors also thank the staff at the University of Lausanne (Switzerland) for completing the Rock-Eval®
580 analyses, and they are particularly grateful to Thierry Adate (Institute of Earth Sciences) and Stéphanie Grand
581 (Institute of Earth Surface Dynamics) for their technical and scientific supports. Finally, we thank the
582 anonymous Reviewers for their useful comments.

583 **Funding**

584 This research was funded by the Ministero dell'Istruzione, dell'Università e della Ricerca through the PRIN
585 2010-2011 project (grant number 2010AYKTAB006; project leader C. Baroni), the project of strategic interest
586 NEXTDATA (PNR National Research Program 2011-2013; project leader A. Provenzale CNR-ISAC). This
587 work has besides benefited from the framework of the COMP-HUB Initiative (unipr), funded by the
588 'Departments of Excellence' program of the Italian Ministry for Education, University and Research (MIUR,
589 2018-2022).

590

591

592

593 **References**

- 594 Albrecht R, Sebag D and Verrecchia EP (2015) Organic matter decomposition: bridging the gap between
595 Rock-Eval pyrolysis and chemical characterization (CPMAS 13C NMR). *Biogeochemistry* 122, 101–
596 111.
- 597 Avery BW and Bascomb C L (Eds.) (1982) *Soil survey laboratory methods*. Lawes agricultural trust.
- 598 Balesdent J, Girardin C and Mariotti A (1993) Site-Related ¹³C of Tree Leaves and Soil Organic Matter
599 in a Temperate Forest. *Ecology*, 74(6), 1713-1721.
- 600 Bascomb CL (1968) Distribution of pyrophosphate-extractable iron and organic carbon in soils of various
601 groups. *European Journal of Soil Science*, 19(2), 251-268.
- 602 Beckage B, Osborne B, Gavin DG et al. (2008) A rapid upward shift of a forest ecotone during 40 years of
603 warming in the Green Mountains of Vermont. *Proceedings of the National Academy of Sciences*, 105,
604 4197–4202.
- 605 Behar F, Beaumont V and De B. Penteado HL (2001) Rock-Eval 6 technology: performances and
606 developments. *Oil and Gas Science and Technology* 56 (2), 111–134.
- 607 Briffa K and Jones P (1990) Basic chronology statistics and assessment. In Cook, ER and Kairiukstis, LA,
608 editors, *Methods of dendrochronology: applications in the environmental sciences*, Dordrecht: Kluwer,
609 137-152.
- 610 Bollati I, Masseroli A, Mortara G et al. (2019) Alpine gullies system evolution: erosion drivers and control
611 factors. *Two examples from the western Italian Alps*. *Geomorphology* 327, 248–263

612 Burga CA (1991) Vegetation history and palaeoclimatology of the Middle Holocene: Pollen analysis of
613 alpine peat bog sediments, covered formerly by the Rutor Glacier, 2510 m (Aosta Valley, Italy). *Global*
614 *Ecology and Biogeography Letters*, 1, 43–150.

615 Butler DR, Malanson GP, Bekker MF et al. (2003) Lithologic, structural, and geomorphic controls on ribbon
616 forest patterns in a glaciated mountain environment. *Geomorphology*, 55, 203–217

617 Butler DR, Malanson GP, Resler LM et al. (2009) Geomorphic patterns and processes at alpine treeline. In
618 *The changing alpine treeline*, vol. 12, ed. D. Butler, G. Malanson, S. Walsh, S. Fagre, 63–84.
619 Amsterdam: Elsevier.

620 Büntgen U, Esper J, Frank DC, Nicolussi K, and Schmidhalter, M (2005). A 1052-year tree-ring proxy for
621 alpine summer temperatures. *Clim Dynam* 25:141–153. doi:10.1007/s00382-005-0028-1

622 Büntgen U, Frank D, Wilson ROB et al. (2008) Testing for tree-ring divergence in the European Alps.
623 *Global Change Biology*, 14(10), 2443-2453.

624 Büntgen U, Tegel W, Nicolussi K et al. (2011) 2500 years of European climate variability and human
625 susceptibility. *Science* 331:578–582

626 Chersich S, Rejšek K, Vranová V et al. (2015) Climate change impacts on the Alpine ecosystem: an
627 overview with focus on the soil. *Journal of Forest Science*, 61(11), 496-514.

628 Coppola A, Leonelli G, Salvatore MC et al. (2012) Weakening climatic signal since mid-20th century in
629 European larch tree-ring chronologies at different altitudes from the Adamello-Presanella Massif
630 (Italian Alps). *Quaternary research*, 77(3), 344-354.

631 Coppola A, Leonelli G, Salvatore MC et al. (2013) Tree-ring-based summer mean temperature variations in
632 the Adamello-Presanella Group. *Clim Past* 9:211–221

633 Corona C, Guiot J, Edouard JL et al. (2010) Millennium-long summer temperature variations in the
634 European Alps as reconstructed from tree rings. *Clim Past* 6:379–400

635 Cremaschi M and Rodolfi G (1991) *Il suolo - Pedologia nelle scienze della Terra e nella valutazione del*
636 *territorio*. La Nuova Italia Scientifica, Roma.

637 D'Arrigo, R.D., Wilson, R., Liepert, B., Cherubini, P., 2008. On the “Divergence Problem” in Northern
638 Forests: A review of the tree-ring evidence and possible causes. *Glob. Planet. Change* 60, 289–305.
639 <https://doi.org/10.1016/j.gloplacha.2007.03.004>

640 D'Amico ME, Calabrese F and Previtali F (2009) Suoli di alta quota ed ecologia del Parco Naturale del Mont
641 Avic (Valle d'Aosta). *Studi Trentini di Scienze Naturali*, 85, 23-37.

642 D'Amico ME, Catoni M, Terribile F et al. (2016) Contrasting environmental memories in relict soils on
643 different parent rocks in the south-western Italian Alps. *Quaternary International*, 418, 61-74.

644 D'Amico ME, Freppaz M, Leonelli G et al. (2015) Early stages of soil development on serpentinite: the
645 proglacial area of the Verra Grande Glacier, Western Italian Alps. *Journal of Soils and Sediments*,
646 15(6), 1292-1310.

647 D'Amico ME, Pintaldi E, Catoni M et al. (2019) Pleistocene periglacial imprinting on polygenetic soils and
648 paleosols in the SW Italian Alps. *Catena*, 174, 269-284.

649 Dal Piaz GV, Gianotti F, Monopoli B et al. (2010) Note illustrative della Carta Geologica d'Italia alla scala
650 1: 50.000, Foglio 091 Chatillon. Servizio Geologico d'Italia, Foglio, 91, 5-152.

651 Dawes MA, Schleppei P, Hättenschwiler S et al. (2017) Soil warming opens the nitrogen cycle at the alpine
652 treeline. *Global change biology*, 23(1), 421-434.

653 Do Nascimento NR, Fritsch E, Bueno GT et al. (2008) Podzolization as a deferralization process: dynamics
654 and chemistry of ground and surface waters in an Acrisol–Podzol sequence of the upper Amazon Basin.
655 *European Journal of Soil Science*, 59(5), 911-924.

656 Egli M and Poulénard J (2016) Soils of mountainous landscapes. *International Encyclopedia of Geography:*
657 *People, the Earth, Environment and Technology: People, the Earth, Environment and Technology*, 1-10.

658 Egli M, Fitze P and Mirabella A (2001) Weathering and evolution of soils formed on granitic, glacial
659 deposits: results from chronosequences of Swiss alpine environments. *Catena*, 45(1), 19-47.

660 Egli M, Merkli C, Sartori G et al. (2008) Weathering, mineralogical evolution and soil organic matter along a
661 Holocene soil toposequence developed on carbonate-rich materials. *Geomorphology*, 97(3-4), 675-696.

662 Egli M, Mirabella A, Sartori G et al. (2006) Effect of north and south exposure on weathering rates and clay
663 mineral formation in Alpine soils. *Catena*, 67(3), 155-174.

664 Egli M, Sartori G, Mirabella A et al. (2009) Effect of north and south exposure on organic matter in high
665 Alpine soils. *Geoderma*, 149(1-2), 124-136.

666 Egli M, Sartori G, Mirabella A. et al. (2010) The effects of exposure and climate on the weathering of late
667 Pleistocene and Holocene Alpine soils. *Geomorphology*, 114(3), 466-482.

668 Freppaz M and Williams MW (2015) Mountain soils and climate change. In: Romeo, R; Vita, A; Manuelli,
669 S; Zanini, E; Freppaz, Michele; Stanchi, Silvia. *Understanding Mountain Soils: A Contribution from*
670 *mountain areas to the International Year of Soils 2015*. Rome: FAO, 106-108.

671 Gale SJ and Hoare PG (1991) *Quaternary Sediments: Petrographic Methods for the Study of Unlithified Rocks*
672 *Belhaven, London*, p. 323

673 Gehrig-Fasel J, Guisan A and Zimmermann NE (2007) Treeline shifts in the Swiss Alps: Climate change or
674 land abandonment? *Journal of Vegetation Science*, 18, 571–582.

675 Gehrig-Fasel J, Guisan A and Zimmermann NE (2008) Evaluating thermal treeline indicators based on air
676 and soil temperature using an air-to-soil temperature transfer model. *ecological modelling*, 213(3-4),
677 345-355.

678 Gerschläuer F, Saiz G, Schellenberger Costa, D et al. (2019) Stable carbon and nitrogen isotopic composition
679 of leaves, litter, and soils of various ecosystems along an elevational and land-use gradient at Mount
680 Kilimanjaro, Tanzania. *Biogeosciences*, 16(2), 409-424.

681 Hagedorn F, Mulder J and Jandl R (2010) Mountain soils under a changing climate and land-use.
682 *Biogeochemistry*, 97(1), 1-5.

683 Harris I, Jones PD, Osborn TJ et al. (2014) Updated high-resolution grids of monthly climatic observations –
684 the CRU TS3.10 Dataset. *Int. J. Climatol.*, 34: 623–642. (doi: 10.1002/joc.3711).

685 Holling CS (1973) Resilience and stability of ecological systems. *Annual review of ecology and systematics*,
686 4(1), 1-23.

687 Holtmeier FK and Broll G (2005) Sensitivity and response of northern hemisphere altitudinal and polar
688 treelines to environmental change at landscape and local scales. *Global ecology and Biogeography*,
689 14(5), 395-410.

690 Holtmeier FK and Broll GE (2007) Treeline advance-driving processes and adverse factors. *Landscape*
691 *online*, 1, 1-33.

692 Holtmeier FK and Broll G (2018) Soils at the Altitudinal and Northern Treeline: European Alps, Northern
693 Europe, Rocky Mountains-A Review. *Insights of Forest Research*, 2(1).

694 Hughes MK (2002) Dendrochronology in climatology—the state of the art. *Dendrochronologia*, 20(1-2), 95-
695 116.

696 Hughes NM, Johnson DM, Akhalkatsi M et al. (2009) Characterizing *Betula litwinowii* seedling microsites
697 at the alpine–treeline ecotone, Central Greater Caucasus Mountains, Georgia. *Arctic, Antarctic and*
698 *Alpine Research*, 41, 112–118.

699 IUSS Working Group WRB (2015) World Reference Base for Soil Resources 2014, update 2015
700 International soil classification system for naming soils and creating legends for soil maps. *World Soil*
701 *Resources Reports No. 106*. FAO, Rome.

702 Jahn R, Blume HP, Asio VB et al. (2006) Guidelines for soil description. FAO.

703 Jenny H (1941) Factors of soil formation: a system of quantitative pedology. McGraw-Hill book company
704 inc., New York.

705 Kjeldahl J (1883) Neue Methode zur Bestimmung des Stickstoffs in organischen Körpern. *J. Anal. Chem.*
706 22, 366–382

707 Klasner FL and Fagre DB (2002) A half century of change in alpine treeline patterns at Glacier National
708 Park, Montana, USA. *Arctic, Antarctic, and Alpine Research*, 34, 49–56.

709 Körner C (1999) *Alpine Plant Life*. Springer, Berlin.

710 Körner C and Paulsen J (2004) A world-wide study of high altitude treeline temperatures. *Journal of*
711 *biogeography*, 31(5), 713-732.

712 Kullman L (2001) 20th century climate warming and tree-limit rise in the southern Scandes of Sweden.
713 *Ambio*, 30, 72–80.

714 Kullman L and Öberg L (2009) Post-Little Ice Age tree line rise and climate warming in the Swedish
715 Scandes: A landscape ecological perspective. *Journal of Ecology*, 97, 415–429.

716 Lafargue E, Marquis F and Pillot D (1998) Rock-Eval 6 applications in hydrocarbon exploration, production,
717 and soil contamination studies. *Oil and Gas Science and Technology* 53 (4), 421–437.

718 Lamb HH (1995) “The little ice age”, *Climate, history and the modern world*, London, Routledge, 464 pp.

719 Legros JP (1992) Soils of Alpine mountains. In *Developments in Earth Surface Processes* (Vol. 2, pp. 155-
720 181). Elsevier.

721 Lehmann J and Kleber M (2015) The contentious nature of soil organic matter. *Nature*, 528(7580), 60.

722 Leonelli G, Masseroli A and Pelfini M (2016) The influence of topographic variables on treeline trees under
723 different environmental conditions. *Physical Geography* 37(1), 56-72.

724 Leonelli G, Pelfini M, Battipaglia G et al. (2009) Site-aspect influence on climate sensitivity over time of a
725 high-altitude *Pinus cembra* tree-ring network. *Climatic Change* 96, 185–201. doi:10.1007/s10584-009-
726 9574-6.

727 Leonelli G, Pelfini M, Morra di Cella U et al. (2011) Climate warming and the recent treeline shift in the
728 European Alps: the role of geomorphological factors in high–altitudes sites. *Ambio*, 40, 264–273.

729 Macias-Fauria M and Johnson EA (2013) Warming-induced upslope advance of subalpine forest is severely
730 limited by geomorphic processes. *Proceedings of the National Academy of Sciences*, 110(20), 8117-
731 8122.

732 Malanson GP, Resler LM, Butler DR et al. (2019) Mountain plant communities: uncertain sentinels?
733 *Progress in Physical Geography* 43 (4):521–543

734 Martinelli LA, Piccolo MDC, Townsend AR et al. (1999) Nitrogen stable isotopic composition of leaves and
735 soil: tropical versus temperate forests. *Biogeochemistry*, 46(1-3), 45-65.

736 Masseroli A, Bollati IM, Proverbio SS et al. (2020) Soils as a useful tool for reconstructing geomorphic
737 dynamics in high mountain environments: The case of the Buscagna stream hydrographic basin
738 (Lepontine Alps). *Geomorphology*, 107442.

739 Masseroli A, Leonelli G, Bollati I et al. (2016) The Influence of Geomorphological Processes on the Treeline
740 Position in Upper Valtellina (Central Italian Alps). *Geogr. Fis. Dinam. Quat.* 39 (2), 171-182, DOI
741 10.4461/ GFDQ 2016.39.16.

742 Matteodo M, Grand S, Sebag D et al. (2018) Decoupling of topsoil and subsoil controls on organic matter
743 dynamics in the Swiss Alps. *Geoderma*, 330, 41-51.

744 Mazepa VS (2005) Stand density in the last millennium at the upper tree-line ecotone in the Polar Ural
745 Mountains. *Canadian Journal of Forest Research*, 35, 2082–2091

746 Melvin, T.M., Briffa, K.R., 2008. A “signal-free” approach to dendroclimatic standardization.
747 *Dendrochronologia* 26 (2008) 71–86. doi:10.1016/j.dendro.2007.12.001.

748 Melvin, T.M., Briffa, K.R., 2014. CRUST: Software for the implementation of Regional Chronology
749 Standardisation: Part 1. Signal-Free RCS. *Dendrochronologia* 32, 7–20.
750 <https://doi.org/10.1016/j.dendro.2013.06.002>

751 Menzel A and Fabian P (1999) Growing season extended in Europe. *Nature* 397, 659.

752 Menzel A, Sparks TH, Estrella N et al. (2006) European phenological response to climate change matches
753 the warming pattern. *Global Change Biology* 12 (10), 1969–1976.

754 Mercalli L, Cat Berro D and Montuschi S (2003) Atlante climatico della Valle d'Aosta, 416 pp. Turin:
755 Società Meteorologica Subalpina.

756 Merkli C, Sartori G, Mirabella A et al. (2009) The soils in the Brenta region: chemical and mineralogical
757 characteristics and their relation to landscape evolution. *Studi Trentini di Scienze Naturali*, 85, 7-22.

758 Ministero delle Risorse Agricole Alimentari e Forestali (1994). *Metodi ufficiali di analisi chimica del suolo,*
759 *con commenti ed interpretazioni.* ISMEA, Roma, 207 pp.

760 Müller M, Schickhoff U, Scholten T et al. (2016) How do soil properties affect alpine treelines? General
761 principles in a global perspective and novel findings from Rolwaling Himal, Nepal. *Progress in Physical*
762 *Geography*, 40(1), 135-160.

763 Nicolussi K, Kaufmann M, Melvin TM et al. (2009) A 9111 year long conifer tree-ring chronology for the
764 European Alps: a base for environmental and climatic investigations. *The Holocene*, 19(6), 909-920.

765 Nicolussi K, Kauffman M, Patzelt G et al. (2005) Holocene tree-line variability in the Kauner valley, central
766 Eastern Alps, indicated by dendrochronological analysis of living trees and subfossil logs. *Veg Hist*
767 *Archaeobot* 14:221–234.

768 Peel MC, Finlayson BL and McMahon TA (2007) Updated world map of the Köppen-Geiger climate
769 classification. *Hydrology and Earth System Sciences*, 11 (5), 1633–1644. doi: 10.5194/hess-11-1633-
770 2007.

771 Pelfini M, Leonelli G, Trombino L et al. (2014) New data on glacier fluctuations during the climatic
772 transition at similar to 4,000 cal. year BP from a buried log in the Forni Glacier forefield (Italian Alps)
773 *Rendiconti Lincei-Scienze Fisiche e Naturali*, 25 (4), 427-437.

774 Phillips JD and Marion DA (2004) Pedological memory in forest soil development. *Forest Ecology and*
775 *Management*, 188(1-3), 363-380.

776 Scapozza C, Lambiel C, Reynard E et al. (2010) Radiocarbon dating of fossil wood remains buried by the
777 Piancabella rock glacier, Blenio Valley (Ticino, Southern Swiss Alps): implications for rock glacier,
778 treeline and climate history. *Permafrost and Periglacial Processes*, 21, 90–96.

779 Schatz AK, Zech M, Buggle B et al. (2011) The late Quaternary loess record of Tokaj, Hungary:
780 reconstructing palaeoenvironment, vegetation and climate using stable C and N isotopes and
781 biomarkers. *Quaternary International*, 240(1-2), 52-61.

782 Schomburg A, Sebag D, Turberg P et al. (2019) Composition and superposition of alluvial deposits drive
783 macro-biological soil engineering and organic matter dynamics in floodplains. *Geoderma*, 355, 113899.

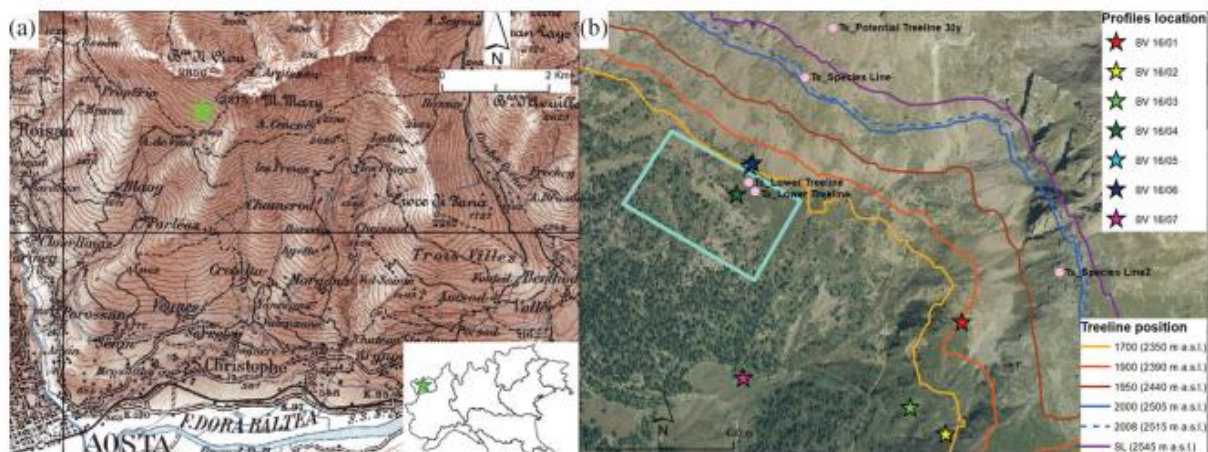
784 Schomburg A, Verrecchia EP, Guenat C et al. (2018) Rock-Eval pyrolysis discriminates soil macro-
785 aggregates formed by plants and earthworms. *Soil Biology and Biochemistry*, 117, 117-124.

786 Sebag D, Verrecchia EP, Cécillon L et al. (2016) Dynamics of soil organic matter based on new Rock-Eval
787 indices. *Geoderma*, 284, 185-203.

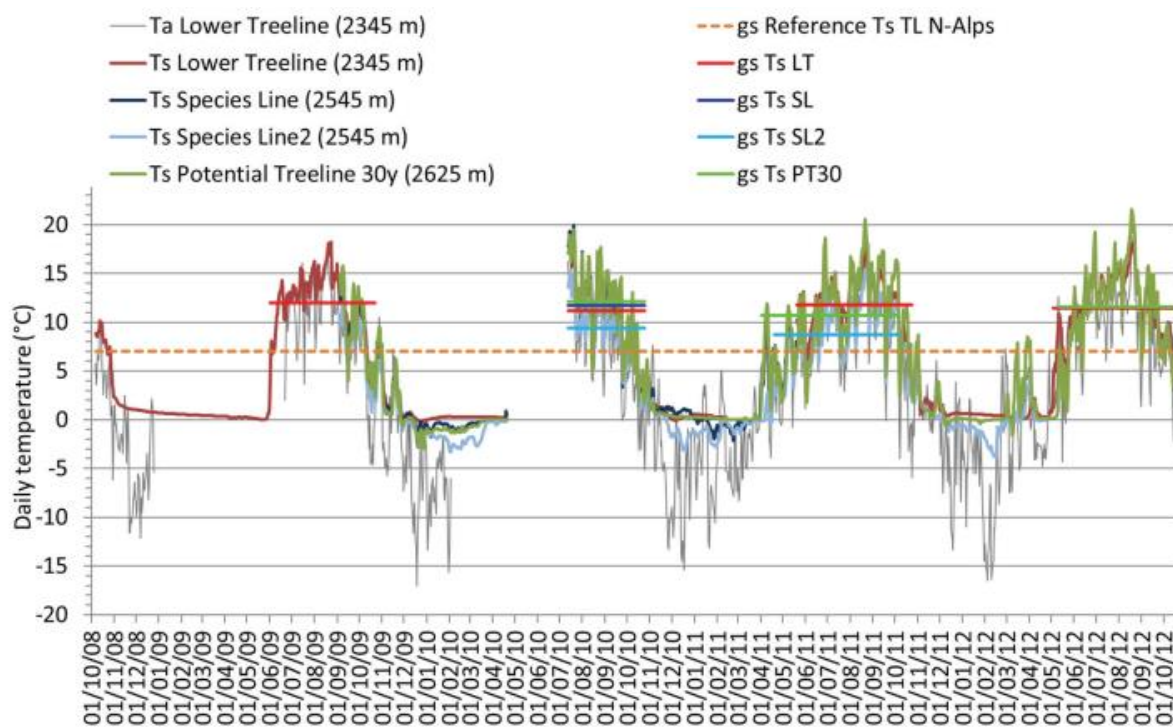
788 Sparks TH and Menzel A (2002) Observed changes in the seasons: an overview. *International Journal of*
789 *Climatology* 22, 1715–1725.

- 790 Stevenson BA, Kelly EF, McDonald EV et al. (2005) The stable carbon isotope composition of soil organic
791 carbon and pedogenic carbonates along a bioclimatic gradient in the Palouse region, Washington State,
792 USA. *Geoderma*, 124(1-2), 37-47.
- 793 Sullivan PF, Ellison SB, McNown RW et al. (2015) Evidence of soil nutrient availability as the proximate
794 constraint on growth of treeline trees in northwest Alaska. *Ecology*, 96(3), 716-727.
- 795 Virtanen R, Luoto M, Rämä T et al. (2010) Recent vegetation changes at the high-latitude tree line ecotone
796 are controlled by geomorphological disturbance, productivity and diversity. *Global Ecology and*
797 *Biogeography*, 19, 810–821
- 798 Vittoz P, Rulence B, Largey T et al. (2008) Effects of climate and land-use change on the establishment and
799 growth of Cembran pine (*Pinus cembra* L.) over the altitudinal treeline ecotone in the Central Swiss
800 Alps. *Arctic, Antarctic, and Alpine Research*, 40, 225–232.
- 801 Walkley A and Black IA (1934) An examination of the Degtjareff method for determining soil organic
802 matter, and proposed modification of the chromic acid titration method. *Soil Sci*, 37(1), 29-38.
- 803 Walther GR, Post E, Convey P et al. (2002) Ecological responses to recent climate change. *Nature* 416, 389–
804 395.
- 805 Wang T, Zhang QB and Ma K (2006) Treeline dynamics in relation to climatic variability in the central
806 Tianshan Mountains, northwestern China. *Global Ecology and Biogeography*, 15(4), 406-415.
- 807 Waroszewski J, Kalinski K, Malkiewicz M et al. (2013) Pleistocene–Holocene cover-beds on granite regolith
808 as parent material for Podzols—an example from the Sudeten Mountains. *Catena*, 104, 161-173.
- 809 Zanelli R, Egli M, Mirabella A et al. (2007) Vegetation effects on pedogenetic forms of Fe, Al and Si and on
810 clay minerals in soils in southern Switzerland and northern Italy. *Geoderma*, 141(1-2), 119-129.
- 811 Zanini E, Freppaz M, Stanchi S et al. (2015) Soil variability in mountain areas. In: Romeo, R; Vita, A;
812 Manuelli, S; Zanini, E; Freppaz, Michele; Stanchi, Silvia. *Understanding Mountain Soils: A*
813 *Contribution from mountain areas to the International Year of Soils 2015*. Rome: FAO, 60-62.
- 814 Zech M, Zech R and Glaser B (2007) A 240,000-year stable carbon and nitrogen isotope record from a loess-
815 like palaeosol sequence in the Tumara Valley, Northeast Siberia. *Chemical Geology*, 242(3-4), 307-318.
- 816
- 817

818 **Figures**

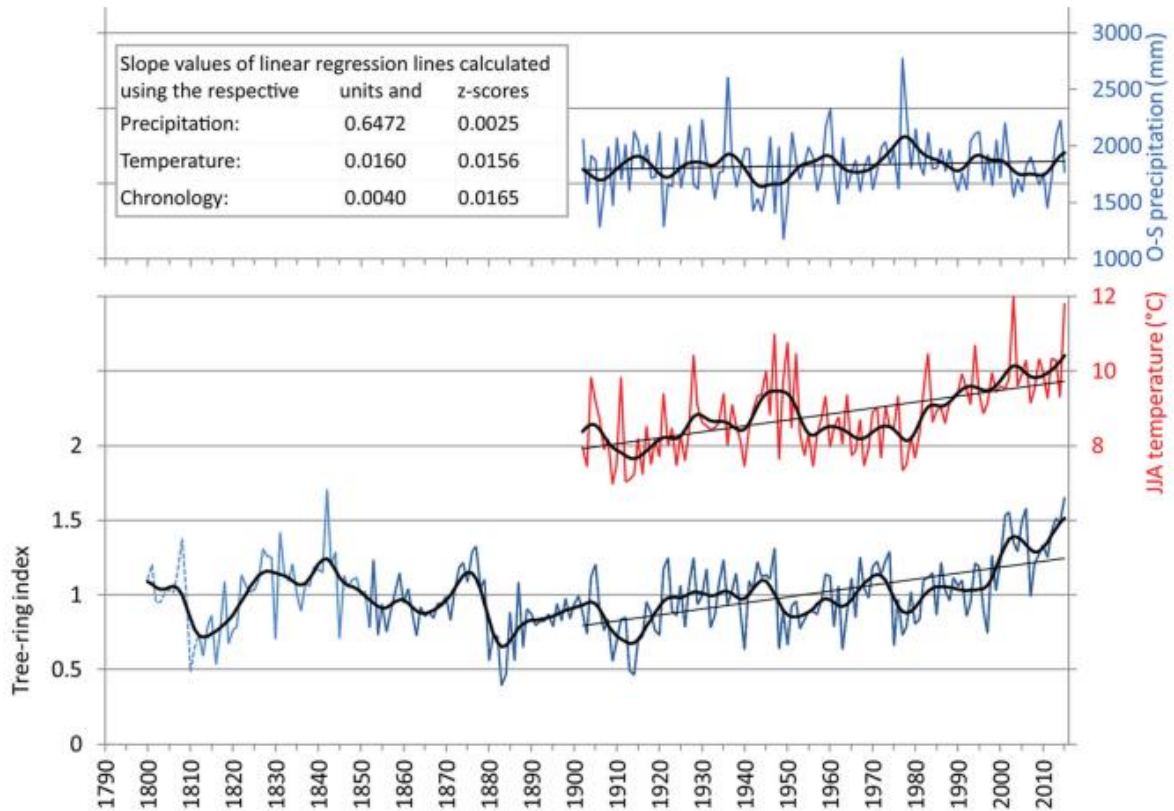


819
 820 Figure 1. (a) Study area and Becca di Viou site location (green star; topographic map from National Geoportal
 821 <http://www.pcn.minambiente.it/GN/>); (b) Locations on the Becca di Viou slope of the soil profiles (stars), of
 822 the dendrochronological sampling area (light blue rectangle) and of the dataloggers (pink dots). In the figure
 823 the treeline positions over 1700–2000 for 50-year time periods, the treeline position in 2008 and the species
 824 line (SL) are also depicted (from Leonelli et al., 2011).
 825
 826
 827

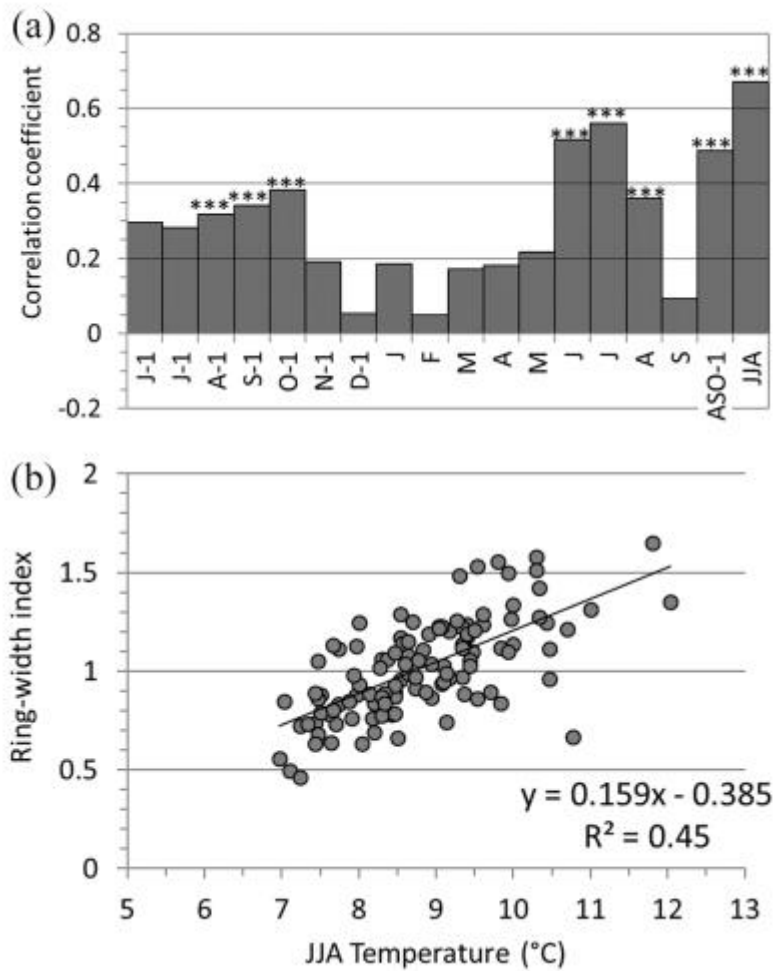


828
 829 Figure 2. Average daily air (Ta) and soil (Ts) temperatures measured at different positions in the treeline belt
 830 between October 2008 and October 2012: Lower Treeline, LT; Species Line, SL; Potential Treeline 30 years,
 831 PT30 (the latter is defined by the altitude with more than 100 days per year with an air temperature > 5 °C over
 832 the 30-yr period 1975–2004; Leonelli et al., 2011); in brackets the altitude of the dataloggers (m a.s.l.)
 833 The horizontal lines depict the average soil temperature of the growing season (gs), defined by the first day
 834 with soil temperature > 3.2 °C (beginning) up to the first day with a soil temperature < 3.2 °C (end of the
 835 growing season; Körner and Paulsen, 2004). The dashed horizontal line depicts the reference soil temperature
 836 for the treelines in the Swiss Alps, i.e. 7 °C (Gehrig-Fasel et al., 2008).

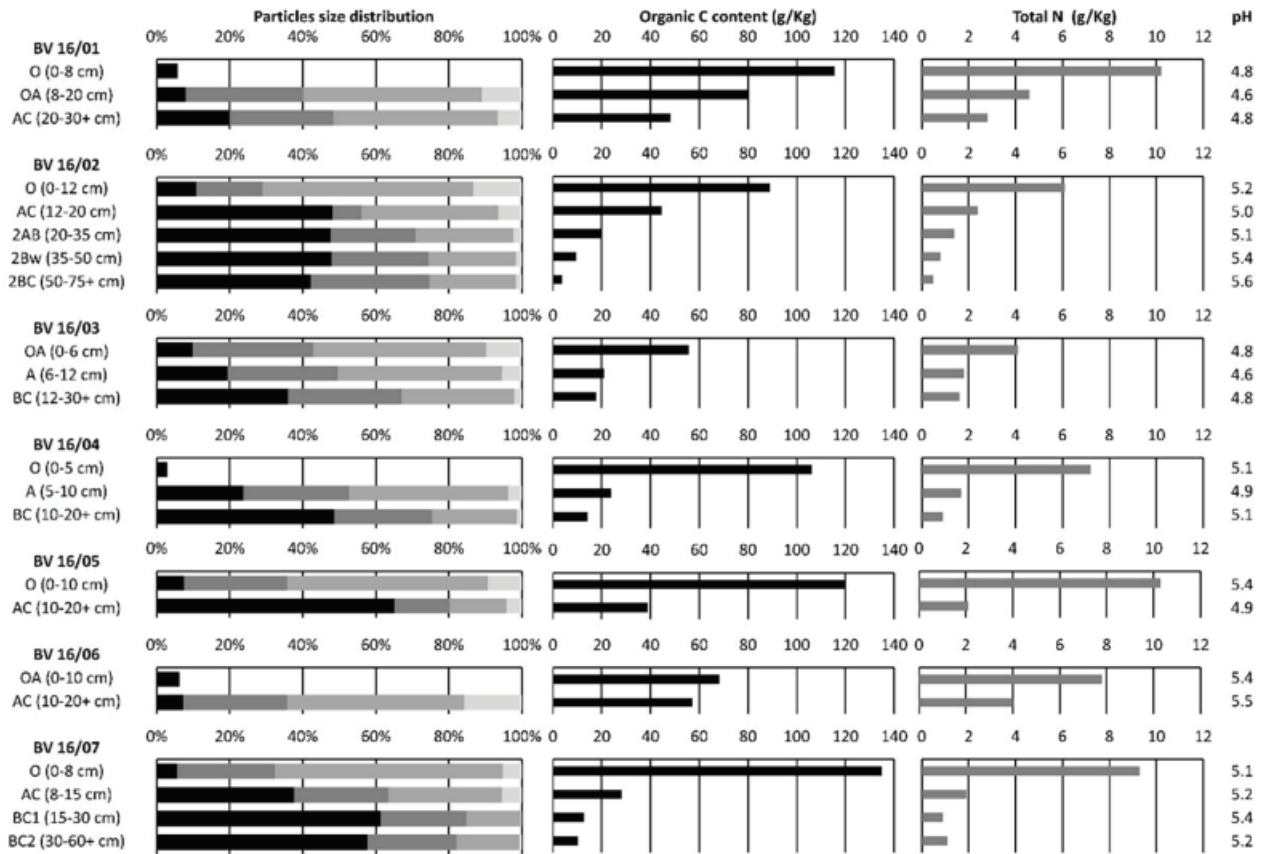
837
838



839
840 Figure 3. At the bottom, the signal-free chronology of the Becca di Viou site over the period 1800-2015 (dark
841 blue line = EPS >0.85 since 1852; light blue = EPS >0.71 since 1812; dashed light blue for the previous period
842 since AD 1800). The graph also depicts the June-to-August mean temperature (JJA; in red) and the October-
843 to-September total precipitations (i.e. a 12-month water year; in blue) over the period 1902-2015.
844 All the series are smoothed with a 20-yr Gaussian low-pass filter with standard deviation set to 4 yr (black
845 lines) and a fitting regression line whose slope value referred to the respective units and to z-scores is reported
846 in the table in the top-left corner.
847

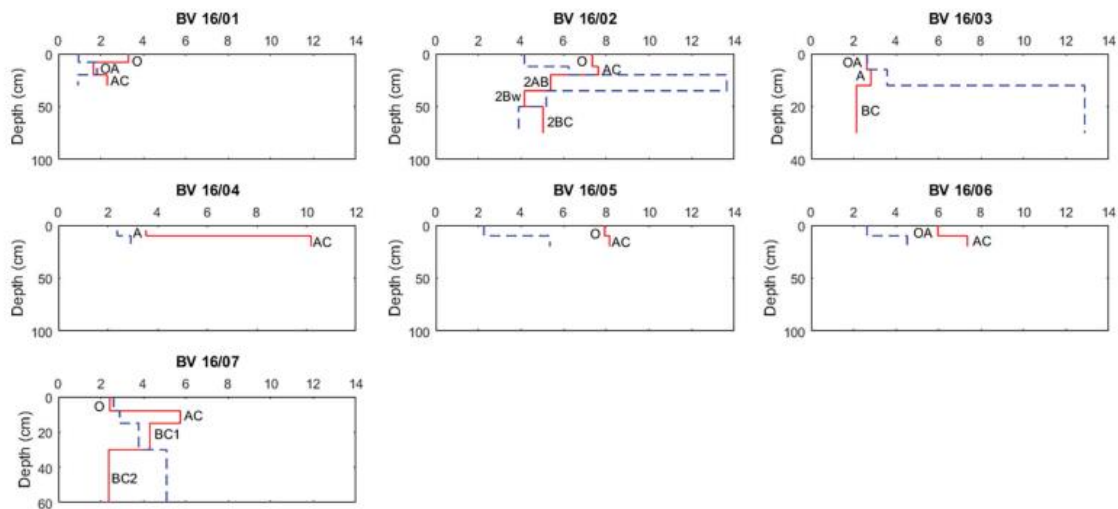


848
 849 Figure 4. (a) Correlation coefficient calculated over the period 1902-2015 between the signal-free chronology
 850 and the monthly temperature variables from June of the previous year to September. *** = $p < 0.001$. (b)
 851 Linear regression of ring-width indices of the signal-free chronology on summer (JJA) temperatures; the
 852 coefficient of determination and the regression equation are also reported.
 853



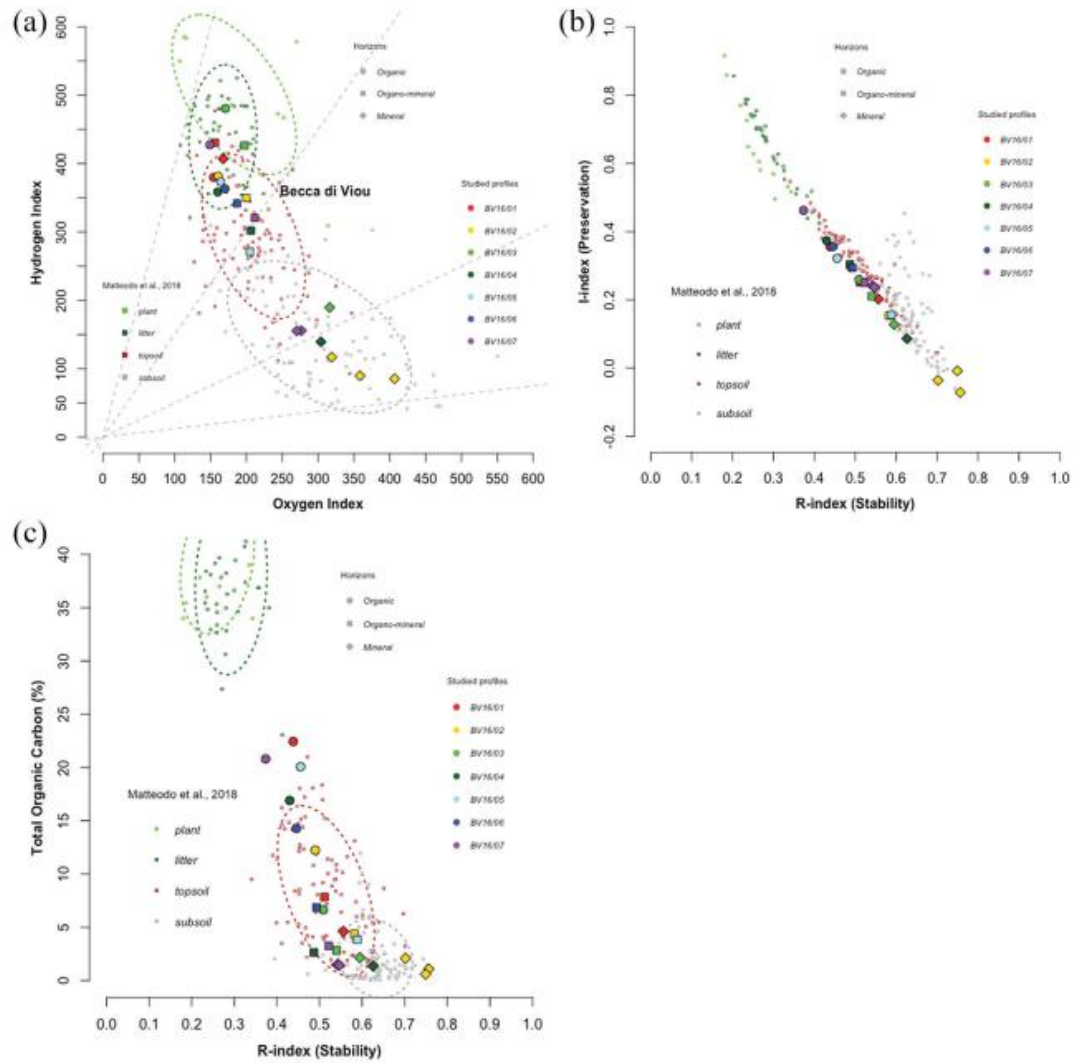
854
855
856
857
858

Figure 5. Particle size distributions, organic C contents (C_{org}), total N contents, and $pH(H_2O)$ values in the studied profiles. In plots of particle size distributions, the gravel, sand, silt, and clay contents are depicted in black, dark grey, grey and light grey, respectively.

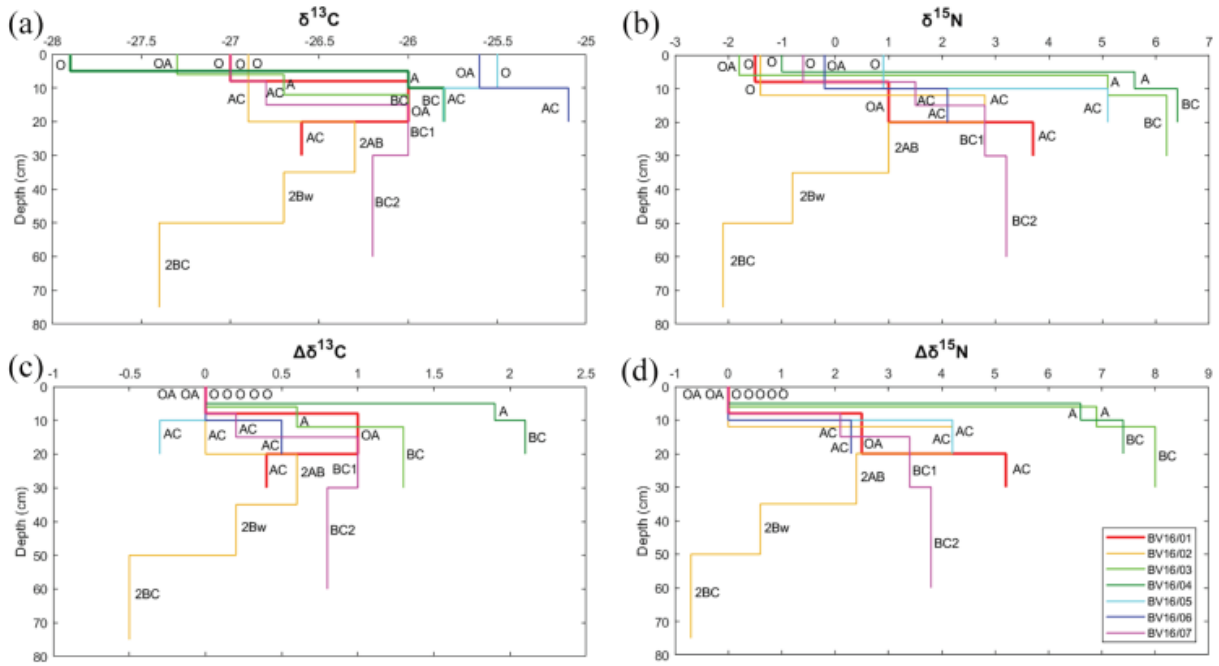


859
860
861
862
863

Figure 6. Variations in the studied profiles of crystalline iron oxides ($Fe_{cry} = Fe_d - Fe_o$, red line; g/Kg) and ammonium oxalate extractable Fe (Fe_o , as a measurement of the “activity” of the iron oxides, blue dotted line; g/Kg). Horizon names are displayed close to the Fe_{cry} curves.



864
 865 Figure 7. (a) HI (mg HC/g TOC)/OI (mg CO₂/g TOC) diagram; (b) I-index/R-index of the studied horizons;
 866 (c) Total Organic Carbon content % (TOC)/R-index of the studied horizon. Shapes refer to the horizon type
 867 (organic, organo-mineral, or mineral) and colors to the profile number. Small colored dots, plotted in the
 868 background for comparison, are from Matteodo et al. (2018)'s dataset composed of 46 soil profiles selected
 869 across various eco-units in the Swiss Alps.
 870



871
 872 Figure 8. (a) $\delta^{13}\text{C}$ (‰) values of studied profiles; (b) $\delta^{15}\text{N}$ (‰) values of studied profiles; (c) $\Delta\delta^{13}\text{C}$ (‰) content
 873 of studied profiles, isotopic enrichment with reference to the first horizon; (d) $\Delta\delta^{15}\text{N}$ (‰) content of studied
 874 profiles, isotopic enrichment with reference to the first horizon.

875

876

Table 1. Site descriptions of the investigated soil profiles. The profile exposure is the same as the slope exposure.

Profile	Elevation (m a.s.l.)	Slope (°)	Slope exposure	Parent material	Landform	Vegetation
BV16/01	2400	10	N	Slope deposits composed of Gneiss and Schists	Upper slope	Treeline ecotone, open stands of <i>Larix decidua</i> and grassland
BV16/02	2340	20	NW	Slope deposits composed of Gneiss and Schists	Upper slope	Treeline ecotone, open stands of <i>Larix decidua</i> and grassland
BV16/03	2300	30	W-NW	Slope deposits composed of Gneiss and Schists	Upper slope	Treeline ecotone, open stands of <i>Larix decidua</i> and grassland
BV16/04	2325	15	W-SW	Slope deposits composed of Gneiss and Schists	Upper slope	Treeline ecotone, open stands of <i>Larix decidua</i>
BV16/05	2365	25	S-SW	Slope deposits composed of Gneiss and Schists	Upper slope	Treeline ecotone, open stands of <i>Larix decidua</i>
BV16/06	2370	25	S-SW	Slope deposits composed of Gneiss and Schists	Upper slope	Treeline ecotone, open stands of <i>Larix decidua</i>
BV16/07	2110	20	S-SW	Slope deposits composed of Gneiss and Schists	Middle slope	<i>Larix decidua</i> woodland

Table 2. Dithionite (d)- and oxalate (o)- extractable contents of Fe and Al. Crystalline iron oxides ($Fe_{cr} = Fe_d - Fe_o$), activity iron index (Fe_o/Fe_d) and podzolization index ($Al_o + 1/2Fe_o$).

Profile	Horizon	Depth (cm)	Al_d (g/Kg)	Fe_d (g/Kg)	Al_o (g/Kg)	Fe_o (g/Kg)	Fe_o/Fe_d	$Fe_{cr} = Fe_d - Fe_o$ (g/Kg)	$Al_o + 1/2Fe_o$ (%)
BV16/01	O	0–8	1.23	4.25	1.02	0.95	0.22	3.30	0.15
	OA	8–20	1.41	3.47	2.70	1.82	0.52	1.65	0.36
	AC	20–30+	2.16	3.23	2.60	0.93	0.29	2.30	0.31
BV16/02	O	0–12	2.40	11.50	2.46	4.16	0.36	7.34	0.45
	AC	12–20	3.10	13.85	2.58	6.23	0.45	7.62	0.57
	2AB	20–35	5.82	19.03	6.01	13.64	0.72	5.39	1.28
	2Bw	35–50	5.73	9.34	5.58	5.18	0.55	4.16	0.82
	2BC	50–75+	5.30	8.92	4.47	3.89	0.44	5.03	0.64
BV16/03	OA	0–6	1.84	5.26	1.43	2.64	0.50	2.62	0.27
	A	6–12	1.35	6.39	2.29	3.58	0.56	2.80	0.41
	BC	12–30+	3.44	15.00	4.19	12.87	0.86	2.13	1.06
BV16/04	O	0–5	0.99	4.86	0.63	<0.90	n.d.	n.d.	n.d.
	A	5–10	1.74	5.92	2.06	2.38	0.40	3.54	0.32
	AC	10–20+	3.41	13.11	2.23	2.92	0.22	10.19	0.37
BV16/05	O	0–10	3.36	10.18	1.56	2.26	0.22	7.91	0.27
	AC	10–20+	3.12	13.50	2.58	5.35	0.40	8.15	0.53
BV16/06	OA	0–10	2.22	8.60	1.12	2.63	0.31	5.97	0.24
	AC	10–20+	4.01	11.87	1.75	4.52	0.38	7.35	0.40
BV16/07	O	0–8	2.55	5.02	1.23	2.60	0.52	2.42	0.25
	AC	8–15	2.12	8.63	1.22	2.89	0.33	5.74	0.27
	BC1	15–30	3.74	8.08	3.17	3.78	0.47	4.30	0.51
	BC2	30–60+	3.79	7.46	4.32	5.09	0.68	2.37	0.69

<: low values approximate to the minor concentration detectable; n.d.: no data.